Soft Matter

RSC Publishing

PAPER

View Article Online
View Journal | View Issue

Cite this: *Soft Matter*, 2013, **9**, 9311

Domain formation on curved membranes: phase separation or Turing patterns?†

E. Orlandini,[a] D. Marenduzzo*[b] and A. B. Goryachev[c]

We study by computer simulations the physics of domain formation on surfaces, as a model for pattern formation on biological membranes. We compare the dynamics predicted by a simple phase separation model for a binary mixture, with that obtained through a conserved Turing-like reaction–diffusion model. Both types of models have been proposed as frameworks for understanding the formation of domains in biological systems. Our main result is that the models can be qualitatively distinguished by analysing the competition dynamics which is set when initialising the system with a number of potential pattern-forming nuclei. Our simulations also suggest that the location of the steady state domains is not uniquely determined by the curvature. This lack of curvature dependence might be advantageous biologically, as it disentangles pattern formation from the mechanics and morphology of the cell membranes. We hope our study will stimulate further experimental work on pattern formation in cells, especially in relation to the cell polarisation problem.

Received 5th March 2013
Accepted 2nd August 2013

DOI: 10.1039/c3sm50650a

www.rsc.org/softmatter

1 Introduction

Reaction–diffusion equations on curved membranes are of high relevance to biology, as they can model pattern formation on cellular membranes,[1] in both prokaryotes and eukaryotes. Examples of applications range from lipid raft formation in eukaryotic cells,[2,3] to protein clustering at bacterial cell poles.[4,5] In some biological systems the membrane curvature has been shown to strongly affect the localisation of individual proteins and protein domains,[5–7] whereas in other cases proteins can deform membranes and such deformations lead to nontrivial protein–protein interactions.[8,9] Therefore, the biophysics of pattern formation on a curved geometry is in general distinct from that on a flat surface.

In order to account for the domains and patterns observed *in vivo*, several models have been proposed in the literature. These models often rely on very different underlying mechanisms, yet lead to superficially similar patterns in the steady state. An important example, on which we focus our analysis here, is that of cellular polarisation, for instance, in budding yeast cells.[10,11] Cell polarity arises through a symmetry-breaking event, as a result of which the cell acquires a directional axis. The onset of directionality, hence polarity, is usually ascribed to the formation of a membrane domain characterized by a distinct composition of lipids and proteins. In budding yeast, symmetry-breaking is associated with the formation of a dense protein cluster containing an activated form of Cdc42 (cell division control protein 42 homolog), a small GTPase of the Rho family, which is involved in the regulation of the cellular cytoskeleton in all eukaryotes. Activated, GTP-bound, Cdc42 concentrates at the site on the cell membrane where the bud will eventually appear.[10,11]

Because there are similarities between polarisation in budding yeast and other biological systems (*e.g.* cells of the immune system, or amphibian eggs), it has been suggested that cell polarisation can be explained through generic, or universal models.[12] A first class of models proposes a bistable underlying dynamics of polarization,[13,14] which is effectively equivalent to thermodynamic phase separation in a binary mixture and is described by the Cahn–Hilliard equation (model B in hydrodynamics parlance). A second class of models suggests a Turing-like mechanism[15] in which a single spatially homogeneous steady state, stable in a well-stirred approximation, is destabilized by diffusion.[1] Our goal here is to study a representative of each of these two prototypical models for domain formation on a curved surface, and ask if we can design an experimental setup which would allow us to differentiate the two types of models. While we consider cell polarisation in yeast as a specific example, this question is very general and important in view of the variety of previously mentioned pattern-formation problems on biological membranes. We hope that the results we present here will motivate further theoretical and experimental work with the aim of testing these classes of models in different contexts.

[a]*INFN and Department of Physics, University of Padova, via Marzolo, 35131 Padova, Italy*

[b]*SUPA, School of Physics and Astronomy, University of Edinburgh, JCMB Kings Buildings, Mayfield Road, Edinburgh, EH9 3JZ, UK. E-mail: dmarendu@ph.ed.ac.uk*

[c]*SynthSys, Centre for Systems Biology, University of Edinburgh, Waddington Building, Mayfield Road, Edinburgh, EH9 3JR, UK*

† Electronic supplementary information (ESI) available. See DOI: 10.1039/c3sm50650a

We shall see that the Turing-like and thermodynamic demixing models lead to very similar results when the initial conditions are random: the domains form and coarsen to leave in a steady state typically only one domain. While the kinetics is different, it would likely be quite hard to decide which model is more appropriate under these conditions. Our main result is that, remarkably, these models can instead be distinguished by a different choice of the initial condition. Thus, when several nuclei of the emerging pattern are implanted in the membrane initially, the dynamics of their competition differ dramatically. For the biologically validated Turing-like model we consider that the competition is solved *via* the rapid growth of one of the domains at the expense of the others, while the bistable model predicts a much slower kinetics, with phase separation effectively being arrested, at least for a very long time. We also find that a bias in the initial condition is more influential with respect to local curvature differences, in determining the final position of the domain on the surface. While perhaps surprising, this fact may be biologically advantageous for the cell, as it makes the pattern forming dynamics robust with respect to transient changes in the cell shape.

Our work is structured as follows. In Section II we review our reaction diffusion algorithm, which is based on finite element techniques; there we also write down the equations of motion for the Turing-like and bistable (phase separation in binary mixture) models. In Section III we present our numerical results, discussing first pattern formation starting from random initial conditions, then nuclei competition, and finally the effect of curvature. Section IV contains a brief discussion of our results and our conclusions.

2 Models and methods

Our goal is to solve a set of reaction–diffusion equations, which we have specified below, on a curved geometry. Although the surface can be in principle arbitrary, in this work we will consider spheres, ellipsoids, and spheres with protrusions (imitating buds) and/or dimples.

Our algorithm was introduced in ref. 16; the reader is referred there for the implementation details. Briefly, we create a triangulation covering the geometry of interest: for surfaces without holes and handles, this can be done through a smooth deformation of the triangulation of a spherical surface (as the topology is the same). Once this is done, we have a network of nodes and links within which we solve the target equations of motion. We note that algorithms very similar to ours have been used previously in the literature to solve reaction–diffusion models, with goals quite distinct from ours.[17–24]

2.1 Cahn–Hilliard dynamics for domain formation in a phase separating binary mixture

We begin by reviewing the equations of motion governing phase separation in a binary mixture; we will refer to this as a binary (occasionally, phase separation) model. This model was used in ref. 13 to study cell polarization. In what follows we refer to the two components as A and B; the minority component, say A, can represent a polarity cluster in the case of budding yeast. We denote the difference in concentrations of A and B as ϕ.

The starting point to derive the dynamic equation of motion for the binary model is the following free energy[25–27] (given in units of thermal energy, k_BT),

$$\frac{\mathscr{F}[\phi]}{k_BT} = \int_S \sqrt{\mathscr{G}}\mathrm{d}s^1\mathrm{d}s^2\left[-\frac{A_0}{2}\phi^2 + \frac{A_0}{4}\phi^4 + \frac{\kappa}{2}g^{\alpha\beta}\partial_\alpha\phi\partial_\beta\phi\right], \quad (1)$$

where $g^{\alpha\beta}$ is the metric tensor,[16,28] which allows among other things the definition of the scalar product and the computation of lengths on the surface (S), $\mathscr{G} = \det(g^{\alpha\beta})$, A_0 is a parameter with units of free energy density, and κ is related to the surface tension of the interface between A-rich and B-rich domains. Note that the double-well structure of the gradient-independent terms in the free energy ensures that the system is bistable ($\phi = -1$ and $\phi = 1$ are the thermodynamically stable states).

The chemical potential corresponding to this free energy is

$$\begin{aligned}\mu = \frac{\delta\mathscr{F}}{\delta\phi} &= -A_0\phi + A_0\phi^3 - \frac{\kappa}{\sqrt{\mathscr{G}}}\partial_\alpha\left(\sqrt{\mathscr{G}}g^{\alpha\beta}\partial_\beta\phi\right)\\ &= -A_0\phi + A_0\phi^3 - \kappa\Delta_{\mathrm{LB}}\phi, \end{aligned} \quad (2)$$

where $\frac{\delta}{\delta\phi}$ denotes the functional derivative, and Δ_{LB} denotes the Laplace–Beltrami operator, which is nothing but the Laplacian on the curved geometry we consider[28] (see Appendix of ref. 16 and references therein for details on our numerical implementation of the Laplace–Beltrami operator in our finite element algorithm). The Cahn–Hilliard dynamics (model B) is a conservation equation for ϕ, where the flux is provided by the gradient of the chemical potential,[25] as follows

$$\frac{\partial\phi}{\partial t} = \Gamma\Delta_{\mathrm{LB}}\mu. \quad (3)$$

Two important things should be noted here. First, we note that although there is no explicit coupling between the order parameter ϕ and the curvature in the free energy, there is an intrinsic coupling through the Laplace–Beltrami operator. Second, with respect to studies of phase separation on curved geometries,[16] here we will restrict ourselves to the case in which the A component is only a small fraction of the membrane composition, typically its total content is 10%. This choice is motivated by the observation that polarized membrane domains normally constitute a small proportion ($\sim$10%) of the cell surface. On a flat geometry, Cahn–Hilliard dynamics leads to the formation of droplets which then grow and coalesce to leave a single droplet of the A phase in the steady state.[13,25]

In the simulations reported below, typical parameters used for the binary model were: $\kappa = 0.5$, $A_0 = 1$, and $\Gamma = 0.33775$. Note that Γ simply rescales time, while κ and A_0 define, together with the local radius of curvature R, a dimensionless number $\sqrt{\kappa/(A_0R^2)}$, which can be viewed as the ratio between the domain interface width and the radius of curvature. In biological systems, this number is below 1. As further discussed below, choosing a different κ such that this dimensionless ratio remains in the biologically relevant range results in dynamics that is qualitatively similar to the one reported here, and therefore variations of κ do not affect our conclusions.

2.2 Conserved Turing-like model of cell polarity

The second model which we consider in this work belongs to the class of Turing-like models with mass-conservation.[29] The Goryachev–Pokhilko[30] model has been recently proposed to explain spontaneous emergence of the cluster of activated Cdc42 GTPase at the future site of bud formation in yeast. While the complete biochemical model comprises eight equations describing the membrane–cytoplasmic shuttling as well as the activation–deactivation dynamics of Cdc42,[31] here we employ a reduced two-variable activator–substrate model which is also derived in ref. 30. We denote the concentration of active GTP-bound (activator) and inactive GDP-bound (substrate) Cdc42 as ϕ and ψ, respectively. The structure of these equations is sufficiently general to be applied as a prototype for other problems in cell polarisation and membrane pattern formation.

The dynamics of the reduced Goryachev–Pokhilko model is governed by the following system of partial differential equations,[30]

$$\begin{aligned}\frac{\partial\phi}{\partial t} &= E_c\alpha\phi^2\psi + E_c\beta\phi\psi - \gamma\phi + D_m\Delta_{LB}\phi \\ \frac{\partial\psi}{\partial t} &= \gamma\phi - E_c\alpha\phi^2\psi - E_c\beta\phi\psi + D_c\Delta_{LB}\psi \\ E_c &= E_c^0\left(1 + \int_S \mathrm{d}s f(\phi(s))\right)^{-1} \\ f(\phi) &= A\phi^2 + B\phi + C\end{aligned} \tag{4}$$

where A, B and C are positive coefficients, which are defined as functions of the specific rate constants of the complete model.[30] In this model, the pattern-forming terms are the nonlinear reaction terms, such as cubic terms proportional to $\phi^2\psi$, typical of activator–substrate models.[32] Another requirement for the emergence of pattern in Turing-like models is a significant disparity $D_c \gg D_m$ between the diffusion coefficient D_m of the slowly diffusing activator (a membrane-bound protein) and the diffusion coefficient D_c of the rapidly diffusing substrate (a typical cytoplasmic protein). The quantity E_c provides a global coupling between the values of ϕ at different places on the membrane and was introduced to specify which part of inactive cytoplasmic GDP-Cdc42 can be converted into active membrane-bound GTP-Cdc42. Finally, one should note that in the system of equations above (which we will refer to as the Turing-like model), the total quantity of active and inactive Cdc42, $\int(\phi + \psi)$, is constant, in contrast to the binary model where it is the order parameter ϕ which is conserved, and the activation reaction is not modelled. This conservation law also renders the model different from the open-system Turing model for pattern formation, which is more common in the literature.[1]

In the simulations reported below, typical parameters used when simulating the Turing-like model were: $D_c = 100$, $D_m = 2.5$, $E_c^0 = 1.7$, $\alpha = 0.000163$, $\beta = 0.000326$, $\gamma = 0.017330$, $A = 0.33$, $B = 0.67$, and $C = 0.01$. This choice is a biologically realistic one, as discussed in ref. 30.

3 Results

We now follow the dynamics of the phase-separating and Turing-like models for domain formation on a curved surface, with the goal of designing ways to discriminate between the predictions of these two models, based on setups which could be realised experimentally. This is important as both models can be used to study cell polarisation, yet the mechanisms proposed to explain pattern-formation are very different.

3.1 Random initial conditions

We start by studying pattern-formation in the two models with random initial conditions. Fig. 1 shows the steady state concentration for GTP-bound Cdc42 (or of the order parameter ϕ in the binary model) on two geometries: a spherical surface (Fig. 1, top), or a sphere with a bump (Fig. 1, bottom). In all cases a single domain is formed.

How is the pattern formed in the two models? To address this question, we show in Fig. 2 snapshots corresponding to successive times during the time evolution. To explore the possible effect of nontrivial and varying curvatures, we report in Fig. 2 the dynamics on an oblate ellipsoid (with ratio between the axes equal to 3 : 3 : 1). In both cases, several droplets, or nuclei, formed initially (Fig. 2, T1 and B1). In the binary model, these droplets grow and we observe coalescence and coarsening (B2 and B3) to leave a single droplet in the end (B4). In the Turing-like model, the dynamics is apparently similar, although initially many more nuclei form (T1), and the coalescence into a single domain appears to be faster (T2–T4, at least with parameters chosen). The dynamics corresponding to Fig. 2 can be seen in full in the ESI, Movies 1 and 2† (for the Turing-like and binary models respectively).

Although qualitatively the coarsening dynamics predicted by the two models look similar, there are quantitative differences, as is apparent from Fig. 3, which shows the evolution of the maximum of the polarity variable ϕ in the two models. In

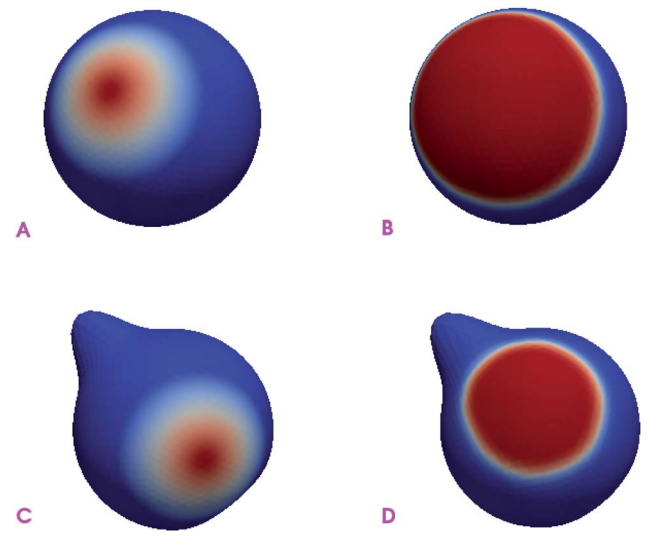

Fig. 1 Steady state configurations found in the Turing-like (A and C), and binary mixture (B and D) models, starting from random initial conditions, on a sphere (A and B) and on a sphere with a bump (C and D). A single domain, or droplet, remains in steady state in all cases. For clarity of visualisation, the colour scale is logarithmic for the Turing-like model (it is instead linear for the binary model).

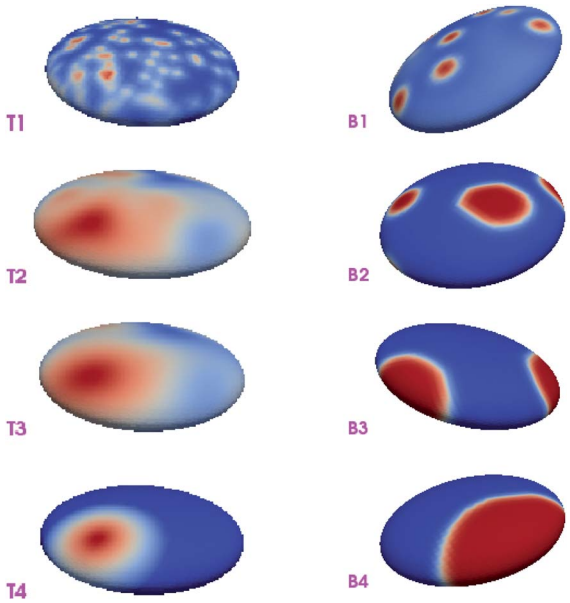

Fig. 2 Snapshots of the dynamics of domain formation on an oblate ellipsoid, for Turing-like (T1–T4) and binary (B1–B4) models. One observes coarsening and coalescence into a single domain in the steady state. For clarity of visualisation, the colour scale is logarithmic for the Turing-like model as in Fig. 1.

particular, one can see that coalescence is accompanied by a decrease in ϕ in the binary model (the A component "spreads out" when two or more droplets merge). In contrast, the formation of a single domain is marked by a dramatic increase in ϕ in the Turing-like model. Fig. 3 also demonstrates that there are subtle differences in the dynamics on surfaces with different geometries (the surface area is the same, and therefore the curves can be directly compared). Another way to analyse quantitative differences in the kinetics is to compute the length scale associated with the domains. This may be defined as the square root of the inverse second moment of the structure factor, the calculation of which on a sphere requires an expansion of the order parameter in spherical harmonics.[19,20] The plots of these quantities (see ESI, Fig. 1 and 2†) reveal that the length scale grows regularly, almost logarithmically, in the binary model, whereas in the Turing-like model pattern formation occurs in a narrow time window. Within this time, the length scale rapidly increases indicating elimination of high spatial frequencies (modes with large wave number). This is followed by a sharp decrease in the length scale suggesting that the pattern undergoes spatial focusing, which is not seen in the binary fluid model. High-resolution experiments probing such early-time dynamics may therefore be able to distinguish the two models. These plots also confirm the intuitive expectation that decreasing κ (related to the interface width and surface tension) slows down the coarsening dynamics, and may lead to trapping into a metastable state.

3.2 Domain competition in the two models

We have thus seen that when starting with random initial conditions both the binary and Turing-like models give rise to a single stable domain, although there are differences in the dynamics through which the steady state is approached. This then begs the question: is it possible to design different initial conditions that could magnify such differences, and render them easier to be observed in an experiment? Can we go as far as arresting coarsening? These are important questions that will arise if we want to devise a way to discriminate which of these two models, if any, applies to a particular membrane pattern formation problem.

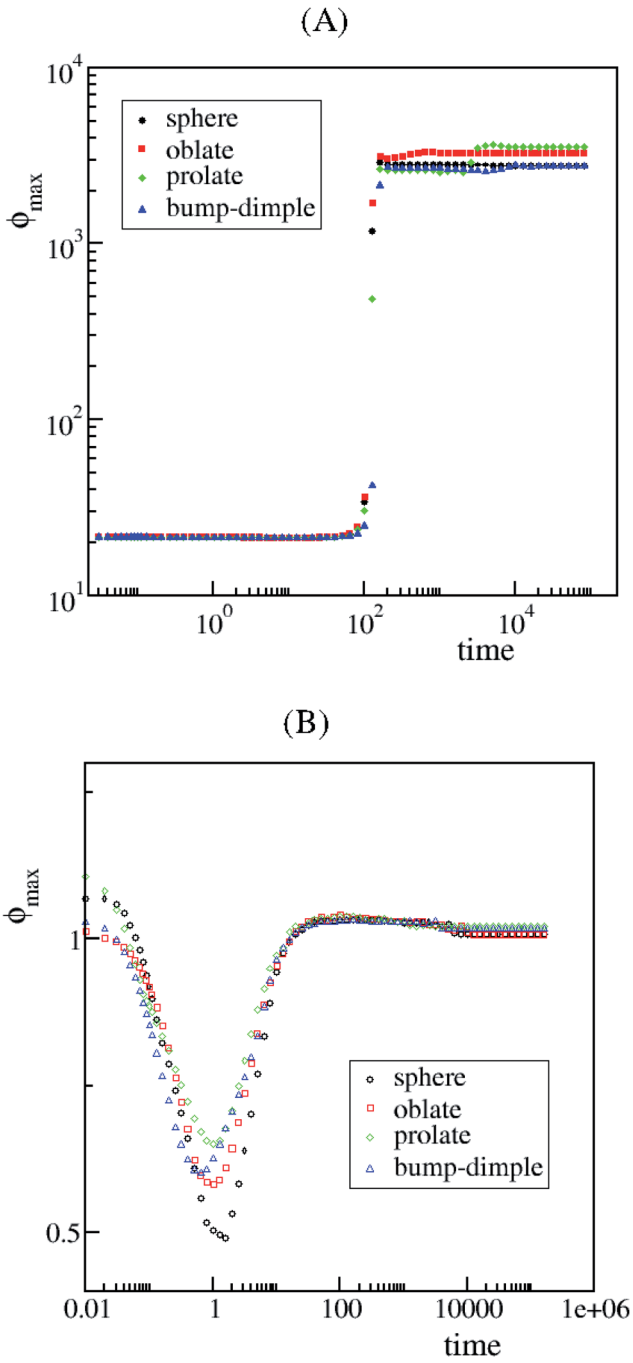

Fig. 3 Time evolution of the maximum of polarity variable ϕ (or A component concentration for binary model), for the Turing-like (A) and binary (B) models on different surfaces (see legend).

In this Section we therefore initialise our simulations differently. We start with two polarity nuclei (large ϕ), in distinct and controlled locations on the membrane and follow the dynamics of their evolution. In other words, we study the competition between rivalling droplets, which were planted into the system. In biological systems, such multiple nuclei emerge naturally due to the random noise and should be detectable in the experiment, for example by means of fluorescent microscopy.[33,34]

Interestingly, our simulations suggest that the observation of competition dynamics between such alternative nuclei may be useful to discriminate between the two types of models considered here.

Fig. 4 shows competition between two droplets initialised around the opposite tips of a prolate ellipsoid (with ratio between the axes equal to 3 : 1 : 1). Left panels follow the evolution of the system for the Turing-like model: it can be seen that one of the droplets shrinks whereas the other grows. The

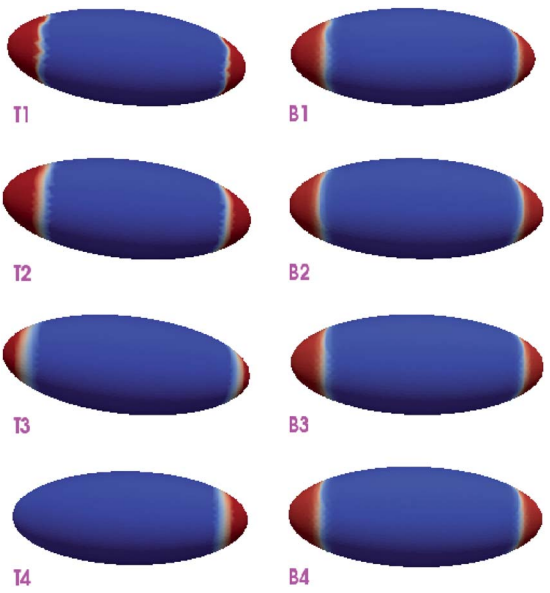

Fig. 4 Snapshots of the dynamics of domain competition on a prolate ellipsoid, for both the Turing-like (T1–T4) and binary (B1–B4) models. Only the Turing-like model leads to the formation of a single droplet in the steady state.

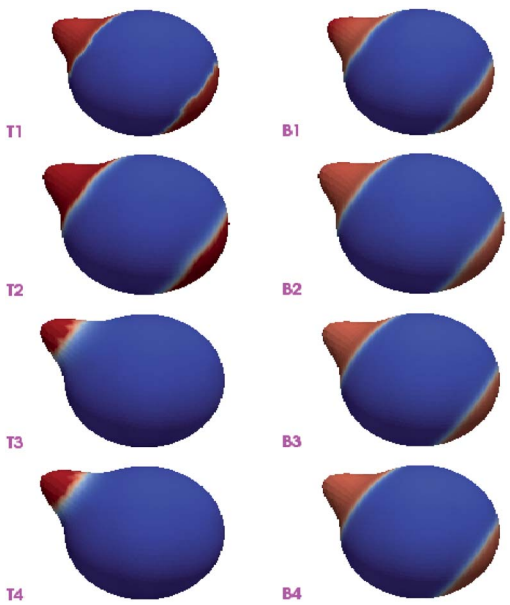

Fig. 5 Same as Fig. 4, but on a sphere with a bump. Snapshots for both the Turing-like (T1–T4) and binary (B1–B4) models are shown. Again only the Turing-like model leads to coalescence into a single domain.

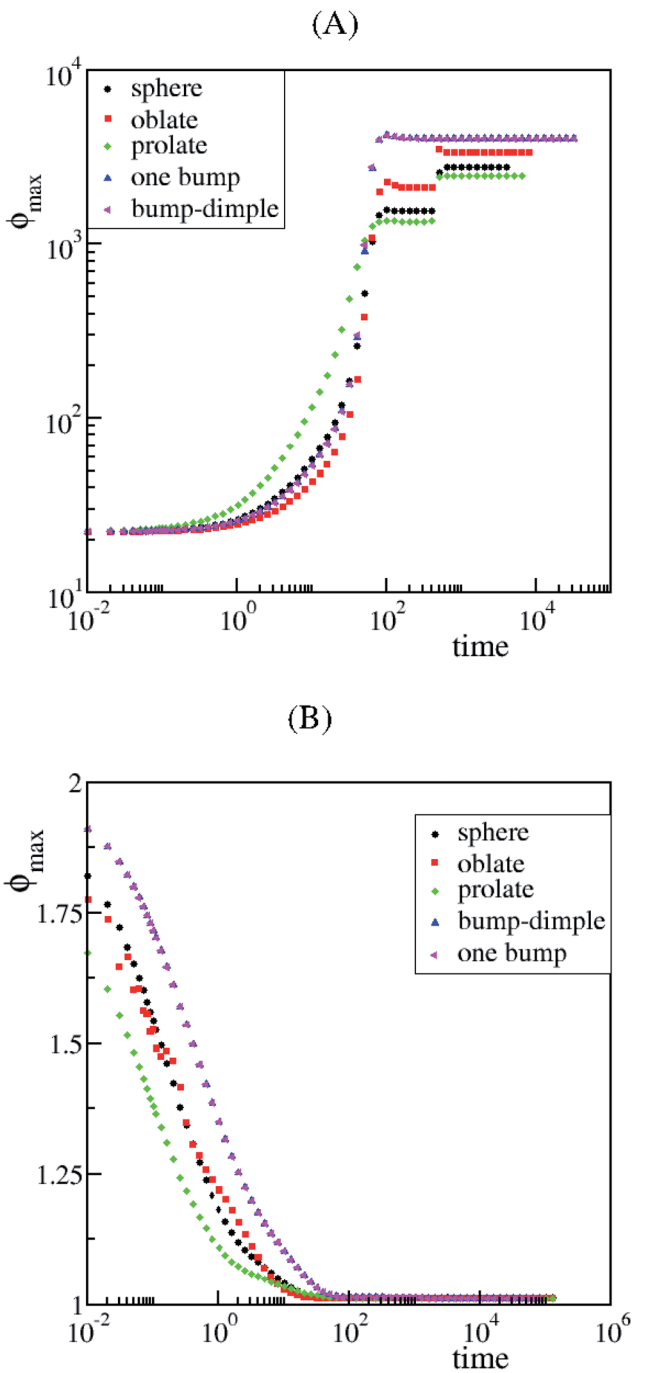

Fig. 6 Time evolution of the maximum of ϕ for the Turing-like (A) and binary (B) models on different surfaces (see legend).

two droplets coalesce without moving towards one another, through an evaporation–condensation mechanism, which is arguably driven by the cytoplasmic shuttling of Cdc42. In our reduced two-variable model of eqn (4) this transport is mimicked by the rapid diffusion of the substrate variable ψ representing an inactive cytoplasmic form of Cdc42. Conversely, the two droplets in the binary model appear to be metastable, and coarsening is not observed. Whether this is a truly arrested or a slowly evolving state cannot be answered within our simulations; certainly the two-domain state is metastable and its lifetime is larger than our simulation times. This is probably due to the fact that coalescence in the binary model requires cross-talk between the tails of two droplets: one domain needs to know about the other's existence to trigger coalescence. Since the flux is proportional to the gradient of chemical potential, the driving force of coalescence becomes exponentially small if the droplets are far apart. Fig. 5 demonstrates domain competition dynamics on a sphere with a bump, with the droplets initialized antipodally. The same behaviour is observed; only the Turing-like model leads to a single domain, which, in this particular case, is localized at the bump. The dynamics corresponding to Fig. 5 can be followed in full in the ESI, Movies 3 and 4.†

This phenomenology is shared between several different geometries: the Turing-like model always results in a single polarization domain at the end of the simulation. For the binary model, however, coarsening sometimes arrests, while proceeding to completion at other times, presumably depending on the initial distance between the nuclei. Fig. 6 shows the dependence of the maximum of ϕ for the two models. The dynamics in the Turing-like model this time shows two stages, the first of which is related to the coalescences of the fading domains (through evaporation–condensation) into a single "winning" domain. Fig. 6A also shows that the dynamics is very similar for the sphere-with-bump-and-dimple and sphere-with-bump geometries, whereas coalescence occurs faster for the prolate geometry and slower for the oblate. Fig. 6B shows that for the binary model the maximum drops from the initial value to 1 in all cases. Unlike in Fig. 3B, the curve is monotonic, because in the binary model no coalescence is observed for the initial condition with two droplets on these geometries. Note that in all cases the droplets are initialised antipodally, so for each given geometry they are positioned as far apart as possible.

3.3 Effect of curvature

In Fig. 2(B1–B4) and 5(T1–T4), a single steady state domain localises at the regions of the highest surface curvature. This is not the case in Fig. 2(T1–T4) (in Fig. 4 domains are initialised at the tip so it is not surprising that the final patterns remain there). While neither of our models incorporate any explicit coupling between the order parameter (polarity variable ϕ) and local curvature, nevertheless there is an intrinsic coupling through the diffusion, or, formally, through the Laplace–Beltrami operator. It is therefore of interest to ask if the curvature directs the dynamics and the steady state location of domains.

A careful analysis shows that the curvature has a weak (if any) effect on the location of the winning, or steady state domain (when there is one, for the binary model). In order to demonstrate this, we have performed simulations for all curved geometries considered (sphere, prolate and oblate ellipsoid, sphere with a bump, with a dimple or both), and studied the

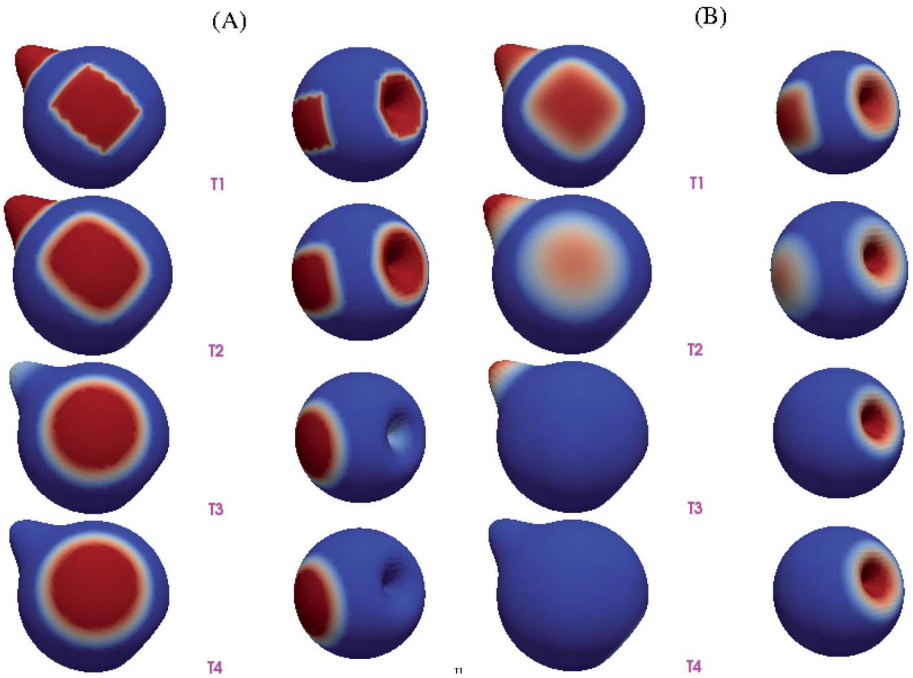

Fig. 7 Snapshots for the time evolution of the Turing-like model on a sphere with a bump and a dimple. The simulations were initialised with three competing GTP-Cdc42 droplets: in (A) the droplet on the side had a slightly larger initial average value of ϕ; in (B) it was the droplet on the dimple which had the initial advantage. The winning domain is always the one favoured by the initial conditions. Note that for each snapshot two views are shown to follow the evolution of all three domains.

competition between domains planted at some selected regions on the membrane. As an example, which is indicative of the generic behaviour, we show in Fig. 7 the competition between three GTP-Cdc42 droplets on a sphere with both a dimple (highly negative curvature) and a bump (highly positive curvature). In Fig. 7A, we have initialised the domain on the side with a slightly larger ($\sim$10% of relative difference) average value of ϕ, whereas in Fig. 7B we have given a small advantage to the domain on the dimple. The results suggest that the initial bias is sufficient to determine where the final domain ends up, thereby showing that, in determining the fate of the pattern, initial conditions are more important than the local curvature.‡ It is possible that in other biological systems an explicit coupling between the order parameter and curvature[16] is justified; we, however, leave such studies for future work.

4 Conclusions

In this work we report on computer simulations of the domain-formation dynamics governed by reaction–diffusion equations on a variety of curved geometries. Here we focus on the comparison between two different types of pattern-forming models that were proposed previously in the literature in the context of cell polarisation. In particular, we first consider a binary mixture model that describes the demixing of a two-component membrane, where one of the components (the minority phase) represents the polarity cluster. We have compared the behavior of this generic thermodynamic model with that of the reduced Goryachev–Pokhilko model that is based on the detailed biochemical mechanism of spontaneous polarity establishment in budding yeast. In this Turing-like model the formation of pattern is due to the interplay between the nonlinear biochemical kinetics and diffusion that takes place on two highly uneven scales, fast in the cytoplasm and slow on the membrane.

Typically, simulations follow the evolution starting from an almost spatially uniform phase with small random fluctuations. We showed that when starting with such random initial conditions, the steady state patterns and dynamics predicted by both models are quite similar: typically we observe the formation of several droplets, which then grow, coalesce and coarsen into a single domain. While there are subtle differences in the kinetics due to the geometry, it is quite difficult to discriminate between the two models in this scenario. However, we find that the dynamics is very different when initialised from preformed competing nuclei of the pattern-forming component. We have shown results pertaining to the competition of two such nuclei: only the Turing-like model leads to a single domain in the end, perhaps due to the more global coupling allowed by the cytoplasmic diffusion route. In contrast, the binary model typically gets stuck into a very long-lived, or possibly even arrested state with two domains. These results suggest that experiments studying the competition between several nuclei might be very useful to dissect the mechanisms leading to pattern formation in biological systems.

Finally, we have seen that the intrinsic curvature we considered (through the Laplace–Beltrami operator which replaces the Laplacian on a curved geometry) is not sufficient to impart a driving force localising the domain to the areas of the given (high or low) curvature; any bias in the initial conditions, even if small, has a much larger effect. This was an unexpected result as the intrinsic curvature has important effects on the phase ordering kinetics;[19] we suggest that this fact may however be advantageous for the cell as it renders the pathway to pattern formation robust to transient changes in the cell's morphology which modify the local curvature at selected locations on the cell membrane.

‡ Note that we cannot exclude that in the absence of any order parameter bias, or when it is much smaller than that considered here, curvature may play a more important role.

References

1 J. D. Murray, *Mathematical Biology*, Springer, New York, 3rd edn, 2004.
2 P. Sens and M. S. Turner, *Phys. Rev. Lett.*, 2011, **106**, 238101.
3 M. S. Turner, P. Sens and N. D. Socci, *Phys. Rev. Lett.*, 2005, **95**, 168301.
4 M. Howard, *J. Mol. Biol.*, 2004, **335**, 655–663.
5 R. Lenarcic, *et al.*, *EMBO J.*, 2009, **28**, 2272–2282.
6 B. J. Peter, *et al.*, *Science*, 2003, **303**, 495–499.
7 N. S. Gov and A. Gopinathan, *Biophys. J.*, 2006, **90**, 454–469.
8 A. R. Evans, M. S. Turner and P. Sens, *Phys. Rev. E: Stat., Nonlinear, Soft Matter Phys.*, 2003, **67**, 041907.
9 T. Idema, S. Semrau, C. Storm and T. Schmidt, *Phys. Rev. Lett.*, 2010, **104**, 198102.
10 E. Bi and H. O. Park, *Genetics*, 2012, **191**, 347–387.
11 A. S. Howell and D. J. Lew, *Genetics*, 2012, **190**, 51–77.
12 A. Mogilner, J. Allard and R. Wollman, *Science*, 2012, **336**, 175–179.
13 A. Gamba, I. Kolokolov, V. Lebedev and G. Ortenzi, *J. Stat. Mech.: Theory Exp.*, 2009, P02019.
14 Y. Mori, A. Jilkin and L. Edelstein-Keshet, *Biophys. J.*, 2008, **94**, 3684–3697.
15 A. M. Turing, *Philos. Trans. R. Soc., B*, 1952, **237**, 37–72.
16 D. Marenduzzo and E. Orlandini, *Soft Matter*, 2013, **9**, 1178–1187.
17 P. Tang, F. Qiu, H. Zhang and Y. Yang, *Phys. Rev. E: Stat., Nonlinear, Soft Matter Phys.*, 2005, **72**, 016710.
18 R. Barreira, C. M. Elliott and A. Madzvamuse, *J. Math. Biol.*, 2011, **63**, 1095–1119.
19 O. Schoenborn and R. C. Desai, *J. Stat. Phys.*, 1999, **95**, 949–979.
20 O. Schoenborn, Phase-Ordering Kinetics on Curved Surfaces, PhD thesis, University of Toronto, 1998.
21 J. Greer, A. L. Bertozzi and G. Sapiro, *J. Comput. Phys.*, 2006, **216**, 216–246.
22 A. Saxena and T. Lookman, *Physica A*, 1999, **133**, 416–426.
23 T. Idema and C. Storm, *Eur. Phys. J. E*, 2011, **34**, 67.
24 C. Varea, J. L. Aragon and R. A. Barrio, *Phys. Rev. E: Stat., Nonlinear, Soft Matter Phys.*, 1999, **60**, 4588–4592.
25 P. Chaikin and T. C. Lubensky, *Principles of Condensed Matter Physics*, Cambridge University Press, Cambridge, 2nd edn, 2000.

26 M. R. Swift, E. Orlandini, W. R. Osborn and J. M. Yeomans, *Phys. Rev. E: Stat., Nonlinear, Soft Matter Phys.*, 1996, **54**, 5041–5052.
27 M. R. Swift, W. R. Osborn and J. M. Yeomans, *Phys. Rev. Lett.*, 1995, **75**, 830–833.
28 E. Kreyszig, *Differential Geometry*, Dover, New York, 1991.
29 M. Otsuji, S. Ishihara, C. Co, K. Kaibuchi, A. Michizuki, *et al.*, *PLoS Comput. Biol.*, 2007, **3**, E108.
30 A. B. Goryachev and A. V. Pokhilko, *FEBS Lett.*, 2008, **582**, 1437–1443.
31 A. B. Goryachev and A. V. Pokhilko, *PLoS Comput. Biol.*, 2006, **2**, 1511–1521.
32 A. Gierer and H. Meinhardt, *Kybernetik*, 1972, **12**, 30–39.
33 A. S. Howell, N. S. Savage, S. A. Johnson, I. Bose, A. W. Wagner, T. R. Zyla, H. F. Nijhout, M. C. Read, A. B. Goryachev and D. J. Lew, *Cell*, 2009, **139**, 731–734.
34 A. S. Howell, M. Jin, C. F. Wu, T. R. Zyla, T. C. Elston and D. J. Lew, *Cell*, 2012, **149**, 322–333.

